Graphical Abstract

This is a specimen a_b title

J.K. Krishnan, Han Thane, William J. Hansen, T. Rafeeq

Highlights

This is a specimen a_b title

J.K. Krishnan, Han Thane, William J. Hansen, T. Rafeeq

- Research highlights item 1
- Research highlights item 2
- Research highlights item 3

This is a specimen a_b title[⋆,⋆⋆]

Sir J.K. Krishnan[a,c,∗,1] (Researcher), Han Thane[b,d], William J. Hansen Jr[b,c,2] (Co-ordinator) and T. Rafeeq[a,c,∗∗,1,3]

[a] *Department of Physics, J.K. Institute of Science, Jawahar Nagar, Trivandrum, 695013, Kerala, India*
[b] *World Scientific University, Street 29, 1011 NX Amsterdam, The Netherlands*
[c] *University of Intelligent Studies, Street 15, Jabaldesh, 825001, Orissa, India*

ARTICLE INFO

Keywords:
quadrupole exciton
polariton
WGM
BEC

ABSTRACT

The advancement and ubiquity of digital networks have fundamentally transformed numerous spheres of human activity. At the heart of this phenomenon, lies the Transmission Control Protocol (TCP) model, whose influence is particularly notable in the exponential growth of the Internet due to its ability to transmit flexibly to any device, through its advanced Congestion Control (CC). Seeking an even more efficient CC mechanism, this work proposes the construction of deep learning neural networks (MLP, LSTM, and CNN) for classifying the level of network congestion. The results attest to models capable of distinguishing, with over 90% accuracy, between moments of high and low degrees of congestion. With this, it becomes possible to differentiate between congestion and random losses, potentially increasing throughput by up to five times in environments with random losses when combined with CC algorithms.
`\beginabstract` …`\endabstract` and `\begin{keyword} ... \end{keyword}` which contain the abstract and keywords respectively. Each keyword shall be separated by a `\sep` command.

1. Introduction

Digital networks, fundamental to the daily lives of modern society, are widely governed by the TCP transport layer. This predominance derives from the broad range of services available on the internet, accessible through a variety of terminals with different architectures. The internet, which has quickly become accessible to around 95% of the global population ITU (2023), operates on a set of rules established by the TCP protocol. Such rules, embedded in operating systems, facilitate the application's data exchange through a series of layered structured services, known collectively as the TCP/IP protocol stack.

A critical element of this stack is the Transport Layer, carried out by Congestion Control (CC). CC is essential to TCP transmissions, adjusting how much data it should transfer in each transmission cycle. A crucial part of CC is the estimation of network congestion level, which, in most available implementations, is performed through losses that have already occurred or variations in delay during data exchange.

In this context, Deep Learning Networks, such as Multilayer Perceptron (MLP) Lippmann (1987), Long Short-Term Memory (LSTM) Hochreiter and Schmidhuber (1997), or Convolutional Neural Network (CNN) Fukushima (1980) emerge as architectures with promising methods for accurately estimating the level of congestion, before infrastructure saturation.

[⋆] This document is the results of the research project funded by the National Science Foundation.
[⋆⋆] The second title footnote which is a longer text matter to fill through the whole text width and overflow into another line in the footnotes area of the first page.

This note has no numbers. In this work we demonstrate a_b the formation Y_1 of a new type of polariton on the interface between a cuprous oxide slab and a polystyrene micro-sphere placed on the slab.

[∗] Corresponding author
[∗∗] Principal corresponding author

`jkk@example.in` (J.K. Krishnan); `wjh@example.org` (W. J. Hansen); `t.rafeeq@example.in` (T. Rafeeq)
`www.jkkrishnan.in` (J.K. Krishnan); `https://www.university.org` (W. J. Hansen); `www.campus.in` (T. Rafeeq)
ORCID(s): 0000-0001-0000-0000 (J.K. Krishnan)

[1] This is the first author footnote, but is common to third author as well.
[2] Another author footnote, this is a very long footnote and it should be a really long footnote. But this footnote is not yet sufficiently long enough to make two lines of footnote text.

1.1. Research questions

Given the above, this work investigates the performance of these AI architectures, directly used in CC, seeking to answer the following research questions (RQ):

- **QP1: (Congestion Learning by Neural Networks)** Investigate the ability of a neural network to learn to classify the degree of congestion in a network connection, based on the occupancy of an output *buffer* in a topology *dumbell*, present in most Internet connections.
  - **QP1.1: (Tolerance to Variation in the Number of Flows)** Evaluate whether the learning model is capable of maintaining its accuracy and effectiveness even when there are significant variations in the volume of traffic (flow) on the network.
  - **QP1.2: (Applicability to Various CC Mechanisms)** Determine whether the learned model can be effectively applied to flows that are controlled by different types of CC mechanisms.
- **QP2: (Identification of the Optimal Dimension for Congestion Classifiers)** Define the ideal combination of measures (such as data components and dimensions) to develop congestion classifiers that are both efficient and accurate.
- **QP3: (Gains from Learning in Random Loss Scenarios)** Examine whether a model developed from a neural network, trained with low-dimensional vectors, can lead to better use of available bandwidth, especially in scenarios characterized by random packet losses.

Based on the research questions outlined, we carried out a broad study through package-level simulations using ns-3 ns3 (2023). The flexibility of ns-3 allows you to explore different versions of TCP, machine learning models and number of flows (up to 40). The simulation results revealed effective performance of neural networks in detecting congestion levels.

This effectiveness also served to apply these models in a practical case: the distinction between random packet losses, a common phenomenon in wireless networks, including Wi-Fi connections and 4G and 5G cellular networks, showing the usefulness of the mechanism with significant improvement in transmission performance in these challenging conditions. To validate our results, we resorted to the use of a specific analytical equation for CC in loss scenarios, proving that the performance of competing protocols is negatively affected in the simulation, according to the literature.

2. Data Mining

To build a training dataset, we implemented a ns3 Traffic Analyzer (AT). The AT performs several simulations of a *dumbbell* topology (Figure 1), a common configuration in network research, which has a central bottleneck and several independent access links. The channels of the stations connected to Router 01 have 2ms delay. In all others, this time is 10ms. The transmission rate is 1Gbs on all channels, with the exception of the one between routers, the bottleneck, which is set to 10, 100, 500 and 1000 Mbps, according to the interested scenarios.

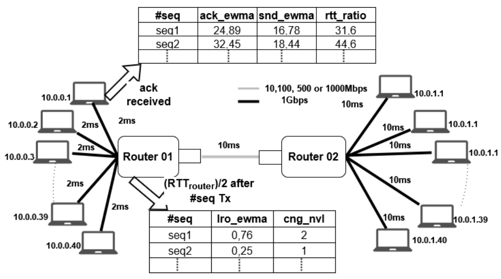

#seq	ack_ewma	snd_ewma	rtt_ratio
seq1	24.89	16.78	31.6
seq2	32.45	18.44	44.6
⋮	⋮	⋮	⋮

#seq	lro_ewma	cng_nvl
seq1	0,76	2
seq2	0,25	1
⋮	⋮	⋮

Figure 1: Topology used to acquire training, validation and tests data and for CC mechanisms evaluation..

Through the dumbbell topology, distributed TCP connections are established. Applications are on terminals connected to Router 01 and TCP servers are on those connected to Router 02. Router 01 10.0.0.2 Terminal connects to terminal 10.1.0.2 of Router 02. Likewise, terminal 10.0.2.2 with the 10.1.2.2; 10.0.3.2 with 10.1.3.2 and so on, until - in case of 80 connections - the last connection, between stations 10.0.79.2 and 10.1.79.2.

The beginning of the connections are spaced of 0.5s to avoid synchronization. Terminal applications were configured to schedule data sending whenever there is space in the *socket* transmission queue. Once such space was identified, each application waits a random time interval t, $0 \leq t < 70$ to exhaust that queue again. This interval was chosen to maintain flows intensity and, at the same time, to make the simulations more realistic in terms of data send randomness.

The training data, for each bottleneck datarate, came from 60 Vegas TCP P2P flow, established on independent links, transporting data capable of saturating the bottleneck, during a 1.5-minute ns-3 simulations [3]. The AT generate two ".csv" files per flow. In the first, the following parameters, inspired by Remmy, are recorded for every ACK received by the sender:

- #seq: Sequence number, present in the ACK packet.
- ack_ewma: Weighted exponential moving average of arrival time between ACK packets.
- snd_ewma: Weighted exponential moving average of the interval between the timestamps present in the respective ACK.
- rtt_ratio: Dividing RTT by RTT_{min}.

To update the second .csv file, whenever a segment is sent in time t, the AT schedules an event at $t + RTT_{router}/2$, where RTT_{router} is the expected RTT between the transmitter and the edge router. During the event handling, the learning target parameters are recorded:

- #seq: Number of seq present in the segment for which the event was scheduled.
- lro_ewma: Weighted exponential moving average of the occupation percentage of the *buffer* of the edge router, to which the transmitter is connected (Router 01 in Figure 1).
- cng_nvl: Network congestion level. If $lro\_ewma <= 40\%$, $cng\_nvl = 1$ or $cng\_nvl = 2$, case $lro\_ewma >= 70\%$.

All moving averages were calculated in microseconds (μs), with a weight of 0.8 for new measurements, in order to prioritize the network momentary state. For training accuracy, the analyzer was configured to record when $lro\_ewma <= 40\%$ or $lro\_ewma >= 70\%$ only. This design seeks robust models in extreme situations, in case of underutilization or overload.

3. Data Processing

The data generated by the (AT) goes through the following stages, before forming the input vectors for the neural networks:

1. *Inner Join* (IJ): The first step consists of generating a table that associates the ack_ewma, snd_ewma and rtt_ratio measurements, with lro_ewma and cng_nvl, through the #seq columns, present in both files collected by the AT.
2. Redundancy Elimination (RE): Lines with identical ack_ewma, snd_ewma and rtt_ratio are discarted, keeping the last record throughout the simulation.
3. Label Balancing (LB): The number of Records with $cng\_nvl = 1$ must be the same as those with $cng\_nvl = 2$. Excess data is disregarded.
4. Attenuators Cut (AC): Records with ack_ewma, snd_ewma and rtt_ratio above the ninetieth percentile (P_{90}) are ignored.
5. Input Normalization (IN): Each of the columns goes through a normalization process, in which its measurements are divided by the maximum value present in it. The normalizers collected from the training data will later be used in all other data that enter the constructed models.

[3]For 10Mbps bottleneck, we execute 11 simulations to take sufficient low congestion data.

Table 1
Neural networks Configuration

epoch:3000; batch size 64; learning rate: 0.0001		
MLP	LSTM	CNN
-Input: 3 dimensional vectors. -Layers: 3 (20 RELU). -Output: Sigmoid.	-Input: Matrix 3x3. -Layers: 2 (each one with 3 LSTM - 30% *dropout*). -Output: Sigmoid.	-Input: Image Vectors 3X3@1. -Convolution:16 maps - 1x3 -Stride: [1,1] -Convolution Output: RELU -Pooling: *maxpooling*, [1,2]. -Flattening: 64 RELU inputs. -Output: Sigmoid.

The resulting table is used to construct a set X, where each element x_i is a vector with components ack_ewma, snd_ewma, rtt_ratio properly treated. Each x_i receives a class $y_i \in Y = \{0, 1\}$, equal to 0 or 1, according to the value of cng_nvl. After the mentioned steps, we reached a set X of 20,000 entries, for each training process, executed per bottleneck datarate cenario.

4. Training Neural Networks - Obtaining the Models

4.1. Overview

The research attained its objectives using twelve models, varying the ARN (MLP, LSTM, CNN), whose specifications are in Table 1, associated with a combination of components (ack_ewma, snd_ewma,rtt_ratio). The type of neural network and the respective input vector components label each model. MLP$_{123}$, for example, refers to the model obtained by the MLP network, receiving the three components as input. LSTM$_{13}$ means model obtained by the LSTM neural network, receiving as input (ack_ewma,rtt_ratio); CNN$_{23}$ to CNN, which receives (snd_ewma,rtt_ratio).

Accuracy, Error, Precision, Recall, and F1, obtained from the *Receiver operating characteristics* (ROC) analysis [4], will be used to compare the models extracted from learning networks. The ROC space is constructed from a Cartesian plane, with the abscissa and ordering associated, respectively, with the rates of false positives, or *False Positive Rate* (FPR), and true positives, or *True Positive Rate* (TPR), for a data set offered to the model.

4.2. Training Vector Transformations

For each of the ARNs, there was a need to transform the vectors from the set X. Transformations description uses three-dimensional vectors, with the components ack_ewma, snd_ewma, and rtt_ratio, as it is analogous to those with one or two components. Regarding MLP, for example, the transformation was direct, without more elaborated rearrangement (Figure 2a).

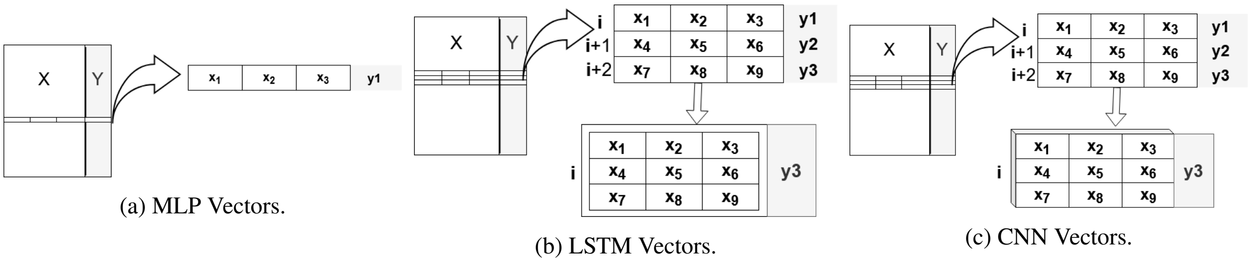

(a) MLP Vectors. (b) LSTM Vectors. (c) CNN Vectors.

Figure 2: NNA data transformations.

The ARN based on LSTM and CNN required elaborate transformations. In LSTN, considering that X has m elements, each element x_i ($i + 2 \leq m$), accompanied by two consecutive vectors, will give rise to an entry in the LSTM network, associated with the class of the third sequence vector (Figure 2b). For the CNN architecture, the X vectors were also grouped consecutively by three and later reformatted, forming a kind of “image” of 3x3 pixels with one channel. (Figure 2c). All training was carried out with 3000 epochs, batch size equal to 64, and a learning rate of

[4]http://mlwiki.org/index.php/ROC_Analysis#ROC_Space

0.0001, using the Keras library from the default configuration of the Google Colab environment. 20% of the 40,000 entries were reserved for testing, while the rest were for training and validation.

5. Model Assessment and Selection (QP1)

5.1. Result Analysis - Test Data

Modelo	Acurácia	Erro	Precisão	Recall	F1
MLP_{123}	0.997	0.003	0.997	0.998	0.997
MLP_{13}	0.998	0.002	1.000	0.995	0.998
MLP_{23}	0.998	0.002	1.000	0.995	0.997
MLP_{12}	0.547	0.453	0.388	0.582	0.465
$LSTM_{123}$	0.994	0.006	0.986	1.000	0.993
$LSTM_{13}$	0.994	0.006	0.984	1.000	0.992
$LSTM_{23}$	0.994	0.006	0.985	1.000	0.992
$LSTM_{12}$	0.418	0.582	0.661	0.370	0.475
CNN_{123}	0.994	0.006	0.985	0.999	0.992
CNN_{13}	0.981	0.019	0.959	0.994	0.976
CNN_{23}	0.978	0.022	0.950	0.994	0.972
CNN_{12}	0.502	0.498	0.658	0.419	0.512

Table 2: Metrics on 10Mbps bottleneck.

Modelo	Acurácia	Erro	Precisão	Recall	F1
MLP_{123}	0.998	0.002	0.999	0.996	0.998
MLP_{13}	0.999	0.001	1.000	0.998	0.999
MLP_{23}	0.997	0.003	0.999	0.995	0.997
MLP_{12}	0.571	0.429	0.447	0.589	0.508
$LSTM_{123}$	0.999	0.001	0.997	1.000	0.998
$LSTM_{13}$	0.999	0.001	0.998	0.999	0.999
$LSTM_{23}$	0.999	0.001	0.997	0.999	0.998
$LSTM_{12}$	0.754	0.246	0.648	0.661	0.654
CNN_{123}	0.998	0.002	0.997	0.998	0.998
CNN_{13}	0.996	0.004	0.998	0.990	0.994
CNN_{23}	0.996	0.004	0.999	0.990	0.995
CNN_{12}	0.746	0.254	0.618	0.655	0.636

Table 3: Metrics on 100Mbps bottleneck.

Modelo	Acurácia	Erro	Precisão	Recall	F1
MLP_{123}	0.912	0.088	0.932	0.894	0.913
MLP_{13}	0.902	0.098	0.937	0.876	0.906
MLP_{23}	0.899	0.101	0.911	0.887	0.899
MLP_{12}	0.652	0.348	0.737	0.629	0.679
$LSTM_{123}$	0.894	0.106	0.857	0.927	0.891
$LSTM_{13}$	0.909	0.091	0.903	0.916	0.909
$LSTM_{23}$	0.907	0.093	0.911	0.904	0.908
$LSTM_{12}$	0.605	0.395	0.392	0.689	0.500
CNN_{123}	0.890	0.110	0.850	0.925	0.886
CNN_{13}	0.906	0.094	0.955	0.870	0.911
CNN_{23}	0.906	0.094	0.954	0.872	0.911
CNN_{12}	0.603	0.397	0.369	0.699	0.483

Table 4: Metrics on 500Mbps bottleneck.

Modelo	Acurácia	Erro	Precisão	Recall	F1
MLP_{123}	0.8590	0.1410	0.8690	0.8580	0.8630
MLP_{13}	0.8480	0.1520	0.8650	0.8380	0.8510
MLP_{23}	0.8480	0.1520	0.8520	0.8360	0.8440
MLP_{12}	0.5150	0.4850	0.1700	0.5640	0.2610
$LSTM_{123}$	0.8290	0.1710	0.7880	0.8700	0.8270
$LSTM_{13}$	0.8440	0.1560	0.8570	0.8440	0.8510
$LSTM_{23}$	0.8230	0.1770	0.7910	0.8560	0.8220
$LSTM_{12}$	0.5100	0.4900	0.4090	0.5340	0.4630
CNN_{123}	0.8470	0.1530	0.8370	0.8630	0.8500
CNN_{13}	0.8420	0.1580	0.8530	0.8430	0.8480
CNN_{23}	0.8410	0.1590	0.8520	0.8420	0.8470
CNN_{12}	0.5220	0.4780	0.4460	0.5470	0.4910

Table 5: Metrics on 1000Mbps bottleneck.

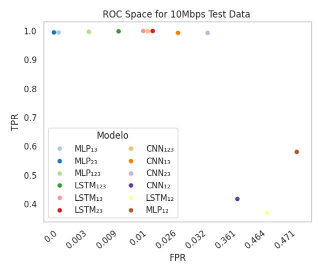

Figure 3: ROC space test Data 10Mbps.

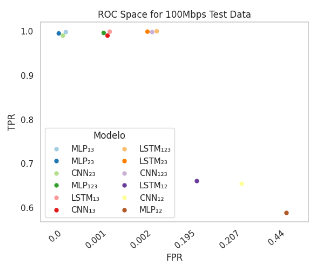

Figure 4: ROC space test Data 100Mbps.

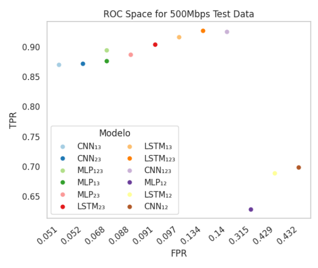

Figure 5: ROC space test Data 500Mbps.

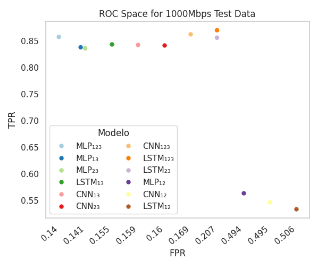

Figure 6: ROC space test Data 1000Mbps.

5.2. Capacidade de generalização dos modelos (QP1.1, QP1.2, QP 2)

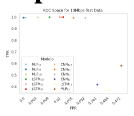
Figure 7: ROC space test Data 10Mbps.

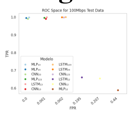
Figure 8: ROC space test Data 100Mbps.

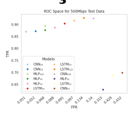
Figure 9: ROC space test Data 500Mbps.

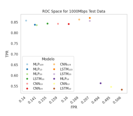
Figure 10: ROC space test Data 1000Mbps.

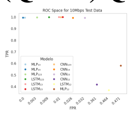
Figure 11: ROC space test Data 10Mbps.

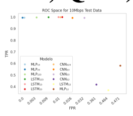
Figure 12: ROC space test Data 10Mbps.

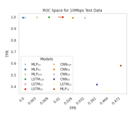
Figure 13: ROC space test Data 10Mbps.

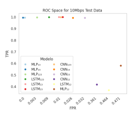
Figure 14: ROC space test Data 10Mbps.

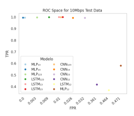
Figure 15: ROC space test Data 10Mbps.

6. Front matter

The author names and affiliations could be formatted in two ways:

(1) Group the authors per affiliation.
(2) Use footnotes to indicate the affiliations.

See the front matter of this document for examples. You are recommended to conform your choice to the journal you are submitting to.

Figure 16: The beauty of Munnar, Kerala. (See also Table 6).

7. Bibliography styles

There are various bibliography styles available. You can select the style of your choice in the preamble of this document. These styles are Elsevier styles based on standard styles like Harvard and Vancouver. Please use BibTEX to generate your bibliography and include DOIs whenever available.

Here are two sample references: See Fortunato (2010). Also refer Fortunato (2010); Newman and Girvan (2004). More citations are here (Fortunato, 2010; Vehlow, Reinhardt and Weiskopf, 2013).

8. Floats

Figures may be included using the command, `\includegraphics` in combination with or without its several options to further control graphic. `\includegraphics` is provided by graphic[s,x].sty which is part of any standard LATEX distribution. graphicx.sty is loaded by default. LATEX accepts figures in the postscript format while pdfLATEX accepts *.pdf, *.mps (metapost), *.jpg and *.png formats. pdfLATEX does not accept graphic files in the postscript format.

The `table` environment is handy for marking up tabular material. If users want to use multirow.sty, array.sty, etc., to fine control/enhance the tables, they are welcome to load any package of their choice and cas-sc.cls will work in combination with all loaded packages.

Table 6
This is a test caption. This is a test caption. This is a test caption. This is a test caption.

Col 1	Col 2	Col 3	Col4
12345	12345	123	12345
12345	12345	123	12345
12345	12345	123	12345
12345	12345	123	12345
12345	12345	123	12345

9. Theorem and theorem like environments

cas-sc.cls provides a few shortcuts to format theorems and theorem-like environments with ease. In all commands the options that are used with the `\newtheorem` command will work exactly in the same manner. cas-sc.cls provides three commands to format theorem or theorem-like environments:

```
\newtheorem{theorem}{Theorem}
\newtheorem{lemma}[theorem]{Lemma}
\newdefinition{rmk}{Remark}
\newproof{pf}{Proof}
\newproof{pot}{Proof of Theorem \ref{thm2}}
```

The `\newtheorem` command formats a theorem in LaTeX's default style with italicized font, bold font for theorem heading and theorem number at the right hand side of the theorem heading. It also optionally accepts an argument which will be printed as an extra heading in parentheses.

```
 \begin{theorem}
  For system (8), consensus can be achieved with
  $\|T_{\omega z}$ ...
    \begin{eqnarray}\label{10}
    ....
    \end{eqnarray}
 \end{theorem}
```

Theorem 1. *For system (8), consensus can be achieved with* $\|T_{\omega z}$ *...*

$$.... \tag{1}$$

The `\newdefinition` command is the same in all respects as its `\newtheorem` counterpart except that the font shape is roman instead of italic. Both `\newdefinition` and `\newtheorem` commands automatically define counters for the environments defined.

The `\newproof` command defines proof environments with upright font shape. No counters are defined.

10. Enumerated and Itemized Lists

cas-sc.cls provides an extended list processing macros which makes the usage a bit more user friendly than the default LaTeX list macros. With an optional argument to the `\begin{enumerate}` command, you can change the list counter type and its attributes.

```
\begin{enumerate}[1.]
\item The enumerate environment starts with an optional
  argument ‘1.’, so that the item counter will be suffixed
  by a period.
\item You can use ‘a)’ for alphabetical counter and ’(i)’ for
  roman counter.
 \begin{enumerate}[a)]
   \item Another level of list with alphabetical counter.
   \item One more item before we start another.
   \item One more item before we start another.
   \item One more item before we start another.
   \item One more item before we start another.
```

Further, the enhanced list environment allows one to prefix a string like ‘step’ to all the item numbers.

```
\begin{enumerate}[Step 1.]
 \item This is the first step of the example list.
 \item Obviously this is the second step.
 \item The final step to wind up this example.
\end{enumerate}
```

11. Cross-references

In electronic publications, articles may be internally hyperlinked. Hyperlinks are generated from proper cross-references in the article. For example, the words Fig. 1 will never be more than simple text, whereas the proper cross-reference `\ref{tiger}` may be turned into a hyperlink to the figure itself: Fig. 1. In the same way, the words Ref. [1] will fail to turn into a hyperlink; the proper cross-reference is `\cite{Knuth96}`. Cross-referencing is possible in LaTeX for sections, subsections, formulae, figures, tables, and literature references.

12. Bibliography

Two bibliographic style files (`*.bst`) are provided — model1-num-names.bst and model2-names.bst — the first one can be used for the numbered scheme. This can also be used for the numbered with new options of natbib.sty. The second one is for the author year scheme. When you use model2-names.bst, the citation commands will be like `\citep`, `\citet`, `\citealt` etc. However when you use model1-num-names.bst, you may use only `\cite` command.

`thebibliography` environment. Each reference is a `\bibitem` and each `\bibitem` is identified by a label, by which it can be cited in the text:
In connection with cross-referencing and possible future hyperlinking it is not a good idea to collect more that one literature item in one `\bibitem`. The so-called Harvard or author-year style of referencing is enabled by the LaTeX package natbib. With this package the literature can be cited as follows:

- Parenthetical: `\citep{WB96}` produces (Wettig & Brown, 1996).
- Textual: `\citet{ESG96}` produces Elson et al. (1996).
- An affix and part of a reference: `\citep[e.g.][Ch. 2]{Gea97}` produces (e.g. Governato et al., 1997, Ch. 2).

In the numbered scheme of citation, `\cite{<label>}` is used, since `\citep` or `\citet` has no relevance in the numbered scheme. natbib package is loaded by cas-sc with `numbers` as default option. You can change this to author-year or harvard scheme by adding option `authoryear` in the class loading command. If you want to use more options of the natbib package, you can do so with the `\biboptions` command. For details of various options of the natbib package, please take a look at the natbib documentation, which is part of any standard LaTeX installation.

A. My Appendix

Appendix sections are coded under `\appendix`.

`\printcredits` command is used after appendix sections to list author credit taxonomy contribution roles tagged using `\credit` in frontmatter.

CRediT authorship contribution statement

J.K. Krishnan: Conceptualization of this study, Methodology, Software. **William J. Hansen:** Data curation, Writing - Original draft preparation.

References

Fortunato, S., 2010. Community detection in graphs. Phys. Rep.-Rev. Sec. Phys. Lett. 486, 75–174.

Fukushima, K., 1980. Neocognitron: A self-organizing neural network model for a mechanism of pattern recognition unaffected by shift in position. Biological Cybernetics 36, 193–202. URL: https://doi.org/10.1007/BF00344251, doi:10.1007/BF00344251. 0000061.

Hochreiter, S., Schmidhuber, J., 1997. Long Short-Term Memory. Neural Computation 9, 1735–1780. URL: https://ieeexplore.ieee.org/abstract/document/6795963, doi:10.1162/neco.1997.9.8.1735. 0000060 Conference Name: Neural Computation.

ITU, G.C.R., 2023. Global Connectivity Report 2022 - https://www.itu.int/itu-d/reports/statistics/2022/05/29/gcr-chapter-1 acesso em 13/12/23. URL: https://www.itu.int/itu-d/reports/statistics/2022/05/29/gcr-chapter-1.

Lippmann, R., 1987. An introduction to computing with neural nets. IEEE ASSP Magazine 4, 4–22. URL: https://ieeexplore.ieee.org/document/1165576, doi:10.1109/MASSP.1987.1165576. 0000062 Conference Name: IEEE ASSP Magazine.

Newman, M.E.J., Girvan, M., 2004. Finding and evaluating community structure in networks. Phys. Rev. E. 69, 026113.

ns3, 2023. A discrete-event network simulator for internet systems - https://www.nsnam.org - vistado em 13/12/05.

Vehlow, C., Reinhardt, T., Weiskopf, D., 2013. Visualizing fuzzy overlapping communities in networks. IEEE Trans. Vis. Comput. Graph. 19, 2486–2495.

Author biography without author photo. Author biography.

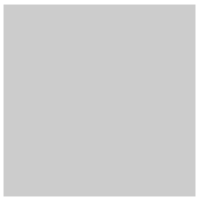

Author biography with author photo. Author biography.

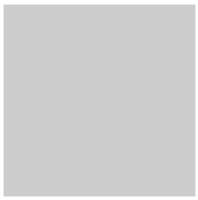

Author biography with author photo. Author biography. Author biography. Author biography. Author biography. Author biography. Author biography. Author biography. Author biography. Author biography. Author biography. Author biography. Author biography.